https://doi.org/10.5194/egusphere-2026-3054
Preprint. Discussion started: 15 June 2026

Earth hummock soils as hot-spots of atmospheric methane uptake in Arctic tundra: a case study from Qeqertarsuaq, West Greenland

Selina Undeutsch[1*], Claudia S. Bruhn[2*], Tino Peplau[3], Sina Plettemeier[2,4], Birgitt Grabellus[1], Susanne Liebner[2,4] and Lars Kutzbach[1]

[1]Department of Earth System Science, Soils of the Climate System, University of Hamburg, Allende Platz 2, Hamburg, Germany
[2]GFZ German Research Centre for Geosciences, Section Geomicrobiology, Telegrafenberg, Potsdam, Germany
[3]Institute of Earth System Sciences, Soil Science Section, Soil Chemistry, Leibniz University Hannover, Herrenhäuser Str. 2, 30419 Hannover, Germany
[4]Institute of Biology and Biochemistry, University of Potsdam, Potsdam, Germany

*These authors contributed equally to this work, Correspondence to: Selina Undeutsch (selina.undeutsch@uni-hamburg.de), Claudia S. Bruhn (claudia.bruhn@gfz.de)

Abstract: Arctic permafrost-affected soils are expected to influence the global greenhouse gas (GHG) budget, although the magnitude of this impact remains uncertain. Methane (CH_4) and carbon dioxide (CO_2) cycling in these environments is largely mediated by soil microorganisms. Cryoturbated soil structures, leading to frost patterned ground phenomena such as unsorted circles, palsas, ice wedges and earth hummocks, are widespread in Arctic landscapes and have been linked to altered GHG fluxes. However, the role of cryoturbated earth hummocks and especially of their microbial community in regulating GHG fluxes remains unexplored. We present one of the first comprehensive assessments of GHG fluxes of cryoturbated earth hummocks in West Greenland, integrating gas flux measurements, soil chemistry and molecular biological analyses. In comparison to less cryoturbated tundra, all investigated earth hummocks exhibited higher CH_4 uptake. Molecular data further revealed an enhanced genetic potential for CH_4 oxidation in hummocks, characterized by a higher relative abundance of atmospheric (high affinity) methanotrophs, while the nearby non-hummocky tundra was dominated by low- and medium-affinity methanotrophs. Consistently, elevated copy numbers of the methanotrophy marker gene *pmoA* indicate that earth hummocks function as hotspots for bacterial methanotrophy. The relatively low pH in the upper horizons of the earth hummock suggests a hydrological decoupling from the minerogenic groundwater, which appears to create favorable conditions for high-affinity atmospheric methanotrophs. Overall, our results identify cryoturbated earth hummocks as strong localized methane sinks and highlight the importance of microtopography in shaping methanotrophic communities and GHG fluxes. These findings underscore the need for a better representation of Arctic tundra microtopography in upscaling GHG fluxes and for an improved mechanistic understanding of methane uptake in cryoturbated tundra soils, particularly about the coupling of hydrology, CH_4 supply, nutrient regime, and pH in regulating methanotrophic activity.

https://doi.org/10.5194/egusphere-2026-3054
Preprint. Discussion started: 15 June 2026

1 Introduction

Permafrost landscapes in the northern hemisphere are storing an estimated 1,000 Pt of organic carbon (OC) in the upper 3 m (Hugelius et al., 2014). With the Arctic warming nearly four times faster than the global average (Rantanen et al., 2022), permafrost-affected areas are projected to shrink by over 40 % by the end of the century (Chadburn et al., 2017). This way, the stored OC can be made available for the metabolism of the soil microbiome, potentially metabolized into greenhouse gases (GHGs), and released into the atmosphere. Arctic landscapes are characterized by extreme small-scale heterogeneity driven by cryoturbation caused by cryopedogenic processes, which are related to the repeated freezing and thawing of the active layer (Burn 1998, Vandenberghe 2007). Cryoturbated permafrost soils (*Turbic Cryosols* according to the World Reference Base for Soil Resources (IUSS Working Group WRB,2022*)*) are estimated to cover 31 % of permafrost soils and to store 44 % of soil organic carbon in the Arctic (Hugelius et al., 2014). These cryoturbation processes can create pronounced microtopography, alter soil hydrology, disturb horizontal soil layering and redistribute soil organic matter (SOM) throughout the soil profile (Van Vliet-Lanoë, 1998; Koven et al., 2009; Ping et al., 2015). Cryoturbation is often accompanied by "frost patterned-ground" features, including sorted and non-sorted circles, stripes and polygons (Washburn, 1956; Lundqvist, 1962; Peterson & Krantz, 2003; Frost et al., 2013; French, 2017). Frost-derived microtopography has already been reported to alter landscape GHG fluxes: mud boils/frost boils in Greenland have shown a potential of methane (CH_4) uptake, albeit lower than other investigated sites in the same area (Jørgensen et al., 2024). Ice wedges in Siberia have been found to be a GHG source, which is explained by altered microbial activity in these microtopographic structures (Park et al., 2024). Other very common non-sorted circles are earth hummocks (hereafter "hummocks"; Mackay, 1980; Washburn, 1980). These dome-shaped structures, typically less than one meter high and one to two meters wide, are formed in fine-grained, water-rich soil materials, which expand during freezing cycles pushing sediment and organic material upwards (Mackay, 1980; Kokelj, 2007). The formation of segregated ice and ice lenses is the primary driver of differential frost heave, which provides the mechanical force necessary to physically uplift, mix, and shape the soil into an earth hummock (Peterson & Krantz, 2008). The micro-topography of hummocks creates a strong physical contrast between the inter-hummock hollows, the top soils of which often remain wet and anoxic, and the uplifted earth hummock crest, the top soils of which are well-drained and aerated (Ruiz-Fernández et al. 2020). The cryoturbation in hummocks results in a relocation of SOM, which leads to increased organic carbon (OC) contents within the hummock soils structures (Wang et al., 2021), through relocation of SOM into deeper soil horizons (Kaiser et al., 2007) with lower microbial activity potentially leads to lower decomposition in the surface-near top soils (Gillespie et al., 2014) and therefore lower GHG release. Crucially, this pronounced topographic and hydrological micro-structure does not only alter substrate burial, but directly dictates the ecological niches available for microorganisms. In particular, bacteria capable of CH_4 oxidation, i.e. methanotrophs, are regulated by environmental constraints. Favorable conditions for aerobic methanotrophy are the availability of oxygen (O), low to moderate pH, and sufficient supply of nutrients such as nitrogen (N) and copper (Cu) (Semrau et al. 2010; D'Imperio et al., 2023). Anoxic conditions and low redox values on the other hand typically favor anaerobic archaea capable of methane production (methanogenesis) (Fetzer et al., 1993; Angel et al., 2011). In waterlogged Arctic soils in Siberia, aerobic methanotrophy was limited to top soil horizons, with only very little methanotrophic activity below (Knoblauch et al., 2008; Murase et al., 2020). The elevated structure of hummocks may, however, expand the aerobic zone of the soil, creating favorable conditions for methanotrophs.

We hypothesize that the physical uplift of the hummock creates a distinct aerobic environment that is well suited for methanotrophic communities, thereby enhancing CH_4 uptake compared to the surrounding tundra. To test this hypothesis, we conducted a comparative field study in the valley Kuup Ilua (Blæsedalen) on Qeqertarsuaq (Disko Island), Western Greenland. We employed an integrative approach combining *in-situ* methane flux measurements throughout the growing

https://doi.org/10.5194/egusphere-2026-3054
Preprint. Discussion started: 15 June 2026

season (July, August, September) with physico-chemical soil profile analysis. Additionally, metabarcoding of the 16S rRNA gene allowed for taxonomic evaluation of the microbial community, particularly the methanotrophic community. Quantitative Polymerase Chain Reaction (qPCR) of the functional genes *pmoA* (coding for a subunit the particulate methane monooxigenase, a marker gene for CH_4 oxidation) and *mcrA* (coding for the methyl coenzyme M reductase, a gene needed for CH_4 production) was used to estimate gene copy numbers of the microbial community driving soil CH_4 fluxes.

2. Material and Methods

2.1 Sampling Locations

Fieldwork was conducted in the glacial valley of Kuup Ilua (Blæsedalen) on Qeqertarsuaq (Disko Island), Western Greenland (69°16' N, 53°28' W). Qeqertarsuaq forms the northern boundary of Disko Bay, a major marine bay on Western Greenland's coast (Kelley et al. 2013), characterized by a Precambrian gneiss ridge overlain by Paleocene basalt flows (Geoffroy et al. 1998; Yde & Knudsen, 2007). The climate is Arctic-maritime, with a mean annual air temperature of -2.7 ± 1.7°C (1992–2021) and annual precipitation of 439 ± 134 mm (2012–2021), according to Hermesdorf et al. (2024). Vegetation is dominated by dwarf shrubs and moss tundra (Hollesen et al. 2015). In late June 2023, the soil of a cryogenic earth hummock (hereafter referred to as H*) was sampled and a vertical soil profile (0–80 cm depth) was described at the earth hummock crest. The soil profile was established in a completely frozen state, preserving frozen soil structures and permitting the *in-situ* description of solid ice components of the soil. The soil of the adjacent inter-hummock hollows was classified as a *Skeletic Cryosol* (Endic). The "Skeletic" designation (IUSS Working Group WRB, 2022) refers to the dominance of coarse rock fragments (>40 % by volume) in the substrate, while the "Endic" qualifier denotes in this context the extremely shallow nature of the soil development on top of larger rock fragments. Extensive soil sampling and detailed characterization were not feasible in this area due to the *Skeletic* and *Endic* characteristics of the soil. A comparison site (non-hummocky tundra or NH) was selected from the surrounding heterogeneous area based on similar soil texture but absence of earth hummock microtopography. This site was characterized as *Mollic Cryosol*. The soil from the non-hummocky tundra NH was previously characterized and described by Peplau et al. (2025). For this study, samples from the NH for biogeochemical analysis were collected one day after the collection of H* samples.

In addition to the H* samples, three more earth hummocks and the directly adjacent inter-hummock hollows were investigated for land-atmosphere methane fluxes without soil sampling, i.e. they were left intact (hereafter "H" for the hummock crests and "IH" for the inter-hummock hollows). All sampling locations are shown in Fig. 1. According to the regional vegetation classification (Figure 1), the study area is characterized as *dry to moist* and *moist tundra* (Gottuk et al., 2025). All gas flux measurement (NH and H) as well as the hummock soil profile (H*) were specifically established within the *moist tundra* reference area. Consequently, differences in methane fluxes and microbial communities can be directly attributed to the specialized physical and chemical niches created by cryogenic hummock formation. All earth hummocks were characterized by a diverse dwarf-shrub community dominated by *Dryas octopetala*, *Salix glauca*, and *Salix arctica*. The ground layer included minor patches of the mosses *Tomentypnum nitens* and *Sphagnum* spp., along with sporadic occurrences of *Empetrum hermaphroditum, Dryas integrifolia*, *Vaccinium uliginosum*, and *Betula nana*. In contrast, the NH was dominated by a dense, uniform moss carpet, primarily consisting of *Tomentypnum nitens* with some *Sanionia uncinata*. Vascular plant cover was sparse, limited to very minor occurrences of *Carex chordorrhiza*, *Equisetum arvense*, *Empetrum hermaphroditum*, and *Betula nana*.

https://doi.org/10.5194/egusphere-2026-3054
Preprint. Discussion started: 15 June 2026

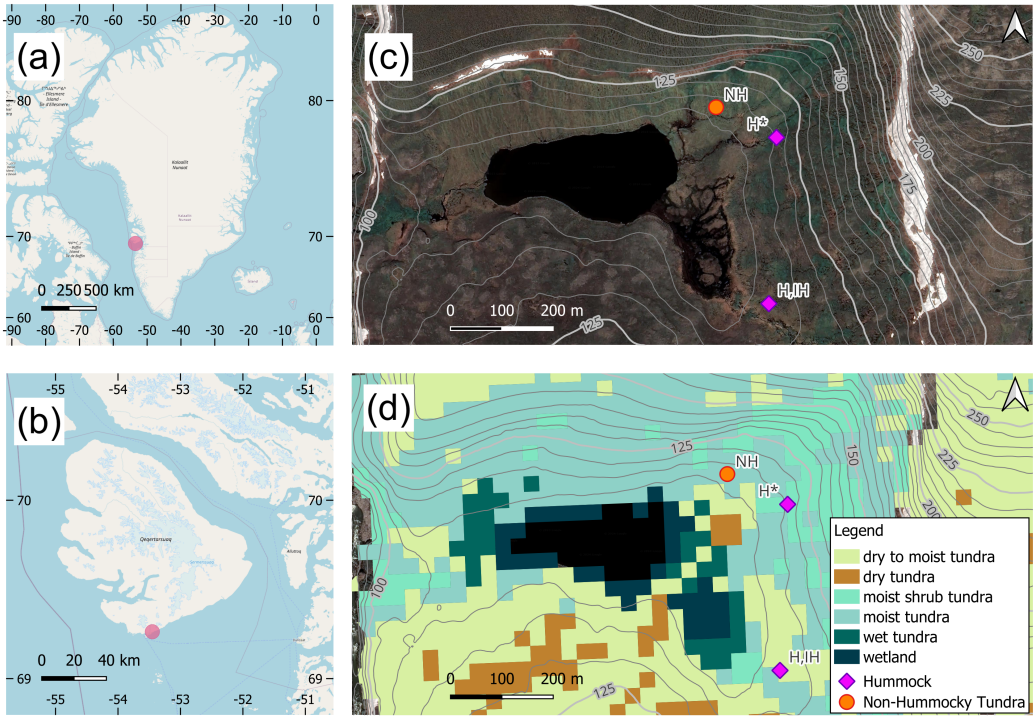

Figure 1: Map of research site Qeqertarsuaq. (a) Map of Greenland with location of island Qeqertarsuaq (Disko Island) (red dot), (b) Location of Kuup Ilua (Blæsedalen, red dot) from ©OpenStreetMap (contributors, 2026), (c) Location of research sites, including hummock (H) and inter-hummock hollow (IH) sites, and H* (pink diamond) and non-hummocky tundra (orange dot) on topographic map from Google Earth, July 15, 2022 (©Google Earth, 2026) and (d) Circumarctic Land Cover Map (Bartsch et al., 2024), adapted from Gottuk et al. (2025).

2.2 Land-Atmosphere Greenhouse Methane Fluxes

Land-atmosphere fluxes of CH_4 were measured using static closed chambers with closed-loop air circulation. The chambers were deployed on 25-cm-diameter PVC collars, installed at the three H and three IH sites, and the NH site, which harbored three replicate collars (Figure 2). Gas concentrations during chamber deployment were monitored in real-time at 1 Hz frequency for 3–5 minutes per measurement using a portable Trace Gas Analyzer (LI-COR LI-7810 $CH_4/CO_2/H_2O$, LI-COR Environmental, Lincoln, USA). Soil temperature was manually measured next to each of the three collars at a depth of 10 cm (DET3R, Voltcraft, Wernberg-Köblitz, Germany). Measurements were conducted weekly between mid-July and late September 2023. To determine the most accurate CH_4 flux, we employed a modified *MATLAB* script (Holl et al., 2026) that simultaneously evaluates both linear and exponential regression for each measurement. Model selection was performed by comparing the Corrected Akaike Information Criterion (AICc) and relative prediction errors, a method that ensures the most suitable model for fitting the data to account for non-linarites caused by chamber saturation (Holl et al., 2026). The final flux was calculated by applying the Ideal Gas Law to the selected rate of concentration change over time, considering measured chamber volume, collar surface area, barometric pressure, and air temperature (Holl et al., 2026). Processes CH_4 flux measurements and soil temperature data, used in this study, is made accessible in supplements (Original data).

https://doi.org/10.5194/egusphere-2026-3054
Preprint. Discussion started: 15 June 2026

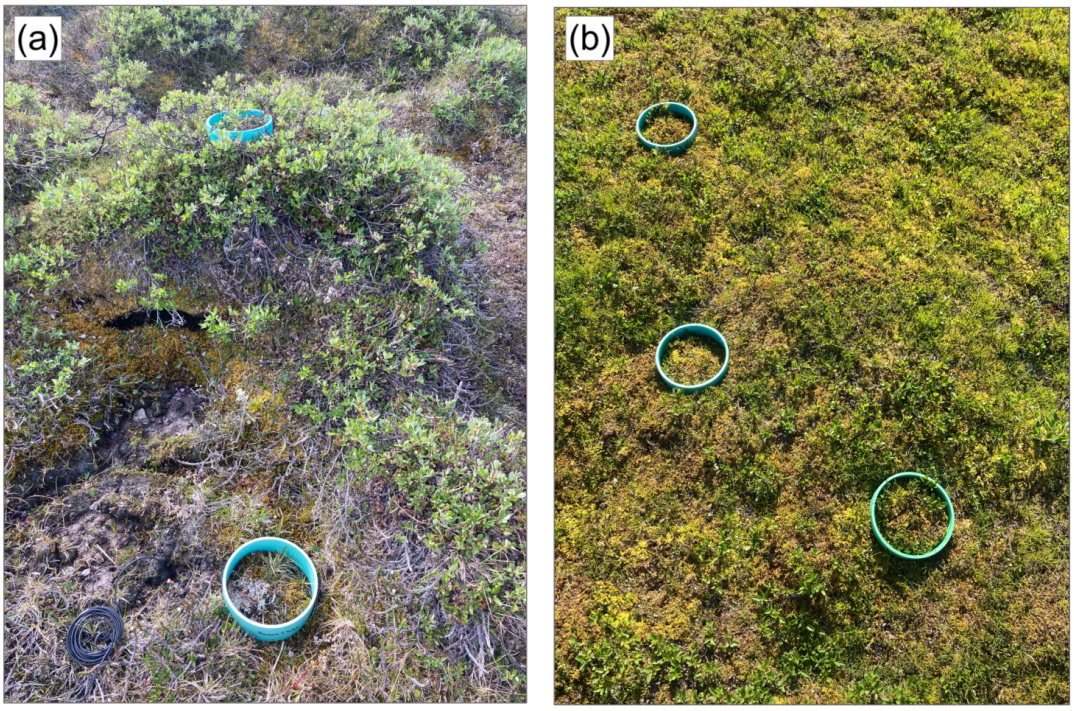

Figure 2: Research Sites. (a) Exemplary earth hummock site, showing one of the three earth hummocks studied for gas fluxes with a measurement collar installed on the crest (example for H), and one on the adjacent inter-hummock hollow (example for IH). (b) Non-hummocky tundra (NH) site (*Mollic Cryosol*), equipped with 3 replicate collars.

2.3 Chemical Soil Analysis

The samples for chemical analyses from NH and H* were frozen at -20 °C immediately after sampling for storage and shipping. At the Leibniz University Hannover, the samples were thawed, freeze-dried, and sieved (< 2 mm) to separate the fine-earth fraction from coarse fragments. The gravimetric water content was determined by relating the mass of the frozen samples to the mass of the freeze-dried samples. All described chemical analyses utilized the fine-earth fraction.

2.3.1 Carbon content and pH

Total carbon (TC) and nitrogen (TN) were quantified using a solid TOC analyser and a nitrogen and protein analyser (soliTOC cube and rapid MAX N, Elementar, Langenselbold, Germany). For samples with TOC > 15%, oxygen dosage was increased to ensure complete combustion. Soil pH was measured in a 1:2.5 (soil:solution by volume) suspension with both distilled water and 0.01 M $CaCl_2$. For organic-rich horizons, the ratio was adjusted to 1:5 or 1:10 to ensure proper suspension.

https://doi.org/10.5194/egusphere-2026-3054
Preprint. Discussion started: 15 June 2026

2.3.2 Water extractable ions

To assess bioavailable nutrients, freeze-dried samples (1–10 g, depending on organic content) were extracted with 20 ml of 0.01 M $CaCl_2$ (1 hour shaking at 200 revolutions per minute and centrifuged at 2500 x g afterwards). The supernatant was analyzed for dissolved organic carbon (DOC) and nitrogen (DN) (LiquiTOC, Elementar Analysesysteme GmbH, Langenselbold, Germany), nitrate (NO_3), sulfate (SO4) and phosphate (PO_4) via Ion Chromatography (IC, 930 IC Flex, Deutsche METROHM GmbH & Co KG, Filderstadt, Germany), and arsenic (As), cadmium (Cd), copper (Cu), iron (Fe), potassium (K), magnesium (Mg), manganese (Mn), and sodium (Na) using inductive coupled plasma optical emission spectroscopy (ICP-OES, Varian 725 ES, Agilent Technologies, Santa Clara, USA).

2.4 Molecular Analysis

For molecular analyses, the NH soil samples were taken from three replicate plots at the same site, approximately 1 m apart from each other. Hummock H* samples were only taken from one plot. The frozen samples were superficially thawed, and smudged sample material was removed from the surface to reveal fresh sample material that was used for subsampling. To account for differences among soil horizons, material was sampled over the full depth of each horizon and pooled into a single Eppendorf tube as an integrated horizon sample. The sample material was either further processed right away or frozen at -60 °C to be processed within two days after sampling.

2.4.1 DNA Extraction

DNA was extracted from approx. 250–290 mg of wet soil using the ZymoBIOMICS MagBead DNA/RNA Kit (Zymo Research, USA). DNA concentration and quality were verified using a Qubit dsDNA BR Assay (Invitrogen; Waltham Massachusetts, USA) and agarose gel electrophoresis before further processing.

2.4.2 Quantitative PCR

The abundance of total bacteria, methanogens, and methanotrophs was quantified using specific qPCR assays, each performed in technical triplicates. For total bacteria, the target gene of the qPCR reaction was the bacterial 16S rRNA gene (primers: Eub341-F/Eub534-R, Muyzer et al., 1993). The graphs for the full analysis of all samples can be viewed in the Supplement. To simplify the presentation of the graphs, we focused on the NH replicate that exhibited the highest 16S rRNA gene copy numbers. This way, functional gene abundances of the NH site were rather overestimated than underestimated, allowing a conservative assessment of gene copy numbers of the H* site in comparison. For methanogens, the *mcrA* gene (coding for the methyl coenzyme M reductase, primers*: mlas-F/mcrA-R,* Steinberg & Regan, 2009) was examined. Primers for detecting aerobic methanotrophs via the *pmoA* gene (coding for a subunit of the particulate methane monooxigenase) have been reported to show different results (Bourne et al., 2001, Knief et al., 2015). For this reason, two primer pairs, pmoA189-F/mb650-R (Bourne et al., 2001) and pmoA189-F/mb661-R (Costello & Lidstrom, 1999), were used and compared with respect to their resulting copy numbers.

https://doi.org/10.5194/egusphere-2026-3054
Preprint. Discussion started: 15 June 2026

2.4.3 16S rRNA Gene Metabarcoding

Amplicon libraries were prepared using the barcoded universal primers Uni515-F and Uni806-R (Caporaso et al., 2011) targeting the V3-V4 regions of the prokaryotic 16S rRNA gene. The barcoded amplicons were purified with a magnetic bead clean-up step using HighPrep PCR – DX (MagBio Genomics Inc., Gaithersburg, USA) according to the manufacturer's protocol. Paired-end sequencing was performed on the Illumina platform (Eurofins, Germany).

Sequencing data was demultiplexed using cutadapt version 3.4 (Martin, 2011) with the parameters -e 0.2 -q 15,15 -m 150 --discard-untrimmed. The sequences were filtered for chimeras, and amplicon sequence variants (ASVs, a proxy for species) were generated with trimmed reads and the DADA2 package version 1.20 (Callahan et al., 2016) in R version 4.4.2 (R Core Team, 2024). For this, the pseudo-pooled approach with the parameters maxN=10, truncQ=2, rm.phix=TRUE and minLen=80 were used. Taxonomic assignment of the ASVs was done using DADA2 and the SILVA database version 138.1 (Quast et al., 2013). Further data processing was performed in R with the help of RStudio (version 2024.09.1+394, Posit team, 2024) and the packages effects (Fox & Weisberg, 2019), ggplot2 (Wickham, 2016), phyloseq (McMurdie & Holmes, 2013), plyr (Wickham, 2011), and vegan (Oksanen et al., 2026). ASVs that were assigned to chloroplasts or mitochondria, as well as low abundance ASVs (singletons and doubletons) were filtered out before normalizing the data to 100 %. The resulting ASVs were then screened for microorganisms reported to be able to pursue methane oxidation or methane production.

3. Results

3.1 Soil Classification and Chemical Analysis

The earth hummock H* soil profile was classified as an *Umbric Turbic Cryosol* (Loamic, Endic, Eutric, Folic) with 9 horizons, according to the World Reference Base for Soil Resources (individual description of horizons: see Appendix Table A1). Morphologically, the profile is defined by active frost churning (Turbic), which has created a heterogeneous mineral subsoil and subducted organic material deep into the profile (Figure 3). The active layer was notably deep (Endic), extending beyond 50 cm, with fine crystalline ice crystals observed at the interface between organic and mineral horizons. Larger and thicker ice lenses accumulated below bigger rock fragments in these soil zones. The top soil was characterized by a well-developed and aerated organic layer profile (Folic, OC > 20 %), exhibiting a distinct decomposition gradient: a relatively undecomposed layer (Oi), a moderately decomposed layer (Oe), and a highly decomposed humic layer (Oa). The organic soil material of the folic horizon was mostly derived from shrub roots and moss remnants. The NH profile was classified as a *Mollic Cryosol* (Loamic, Epic, Hypereutric, Folic, Humic), by Peplau et al. (2025). This soil represents a clearly stratified system with a significantly shallower permafrost table (Epic) and a moss-dominated organic layer. Unlike the H* soil, the NH soil shows no evidence of cryoturbation and maintains an undisturbed regular soil stratigraphy with horizontal orientation of soil horizons.

https://doi.org/10.5194/egusphere-2026-3054
Preprint. Discussion started: 15 June 2026

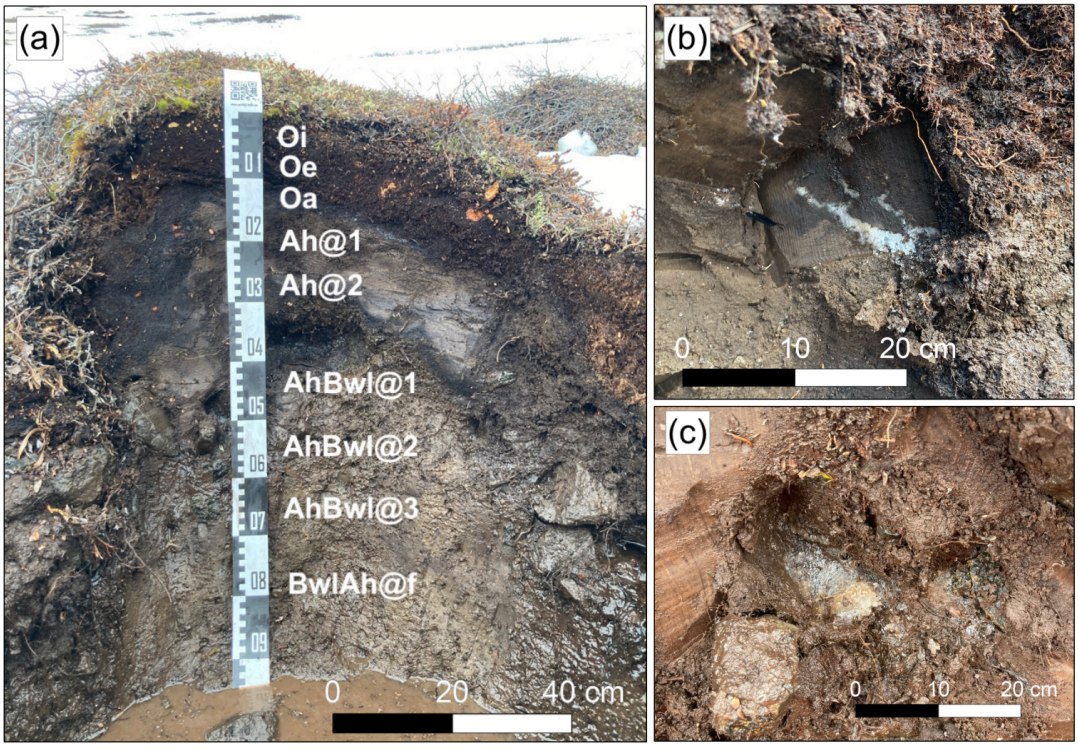

Figure 3, Soil Profile of Earth Hummock (a) Soil profile of the H* profile soil with horizon symbols and description according to the World Reference Base for Soil Resources. (b) Occurrence of segregated ice lenses between organic and mineral layers. (c) Formation of segregated ice lenses at the bottom of a stone of 10 cm diameter.

The pedological analysis of the earth hummock (H*) and non-hummocky tundra (NH) profiles reveal notable differences between soil moisture and chemical properties, specifically acidity and organic matter contents (Figure 4). Despite differences in moisture regimes and pH gradients, both soils exhibit striking similarities in their C and N contents, as well as C:N ratio (Figure 4c, d, e). The surface organic horizons (Oi, Oe, and Oa) of both sites contained nearly identical elemental concentrations. Total C in the organic layers was measured at 34.43 ±12.14 % for H* and 39.61 ±7.75 % for NH (Figure 4c). Similarly, total N concentrations (Figure 4d) were comparable, with H* at 1.41 ± 0.21 % and NH at 1.59 ± 0.33 %. Both profiles displayed a characteristic sharp decline of organic content with depth. In the buried mineral horizons, total C decreased to 2.12 ± 0.79 % in H* (in ~47 cm depth) and 5.68 ± 1.12 % in NH (in ~31 cm depth), while N concentrations followed a similar gradient (0.16 ± 0.06 % and 0.36 ± 0.06 %, respectively).

In contrast to the similar trends in C and N contents, soil moisture diverged sharply especially in deeper horizons depth. While volumetric water content (VWC), seen in Fig. 4b, in the upper organic layers was high for both H* (73.78 ± 5.96 %) and NH (82.16 ± 4.02 %), in H* the mineral subsoil shows a rapid decline in VWC (20.66 ± 1.16 %) below the buried AhBwl horizons (in 47 cm depth). Conversely, the NH soil was significantly more saturated in the lower mineral horizon (44.64 ± 8.29 %) (Figure 4b). The most pronounced divergence in the dataset was observed in soil pH. The H* profiles displayed a strong vertical acidity gradient, transitioning from highly acidic surface horizons (pH 4.54 ± 0.24) to circumneutral values in the underlying mineral layers (pH 6.71 ± 0.16). In contrast, the NH soil exhibited a consistently moderately acidic profile (pH 5.6–5.9) with negligible vertical variation (see also Appendix Table A1).

https://doi.org/10.5194/egusphere-2026-3054
Preprint. Discussion started: 15 June 2026

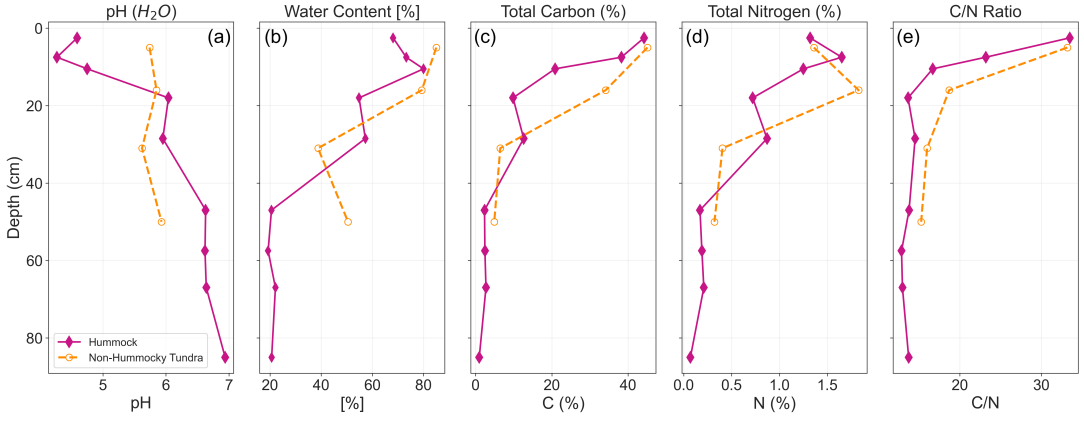

Figure 4: Comparison of vertical soil profiles of physical and chemical properties of Hummock (H*) and Non-Hummocky Tundra (NH). Panels display (a) soil pH (H_2O), (b) gravimetric water content [%], (c) total carbon [%], (d) total nitrogen, and (e) C/N Ratio. Hummock profiles are indicated by pink diamonds and solid lines, and Non-Hummocky Tundra profiles by orange dots and dashed lines).

3.2 Microbial Functional Potential and Community Composition

3.2.1 Vertical distribution of methanotrophs and bacterial abundances

All three plots of NH exhibited similar patterns. To streamline the presentation, only one of the NH plots is shown in detail, but the graphs of the remaining plots are provided in the Appendix (Appendix B Figures B1, B2, B3). The quantitative assessment of the bacterial 16S rRNA gene (a general marker for bacterial abundance) showed more bacteria in all NH plots, while the H* profile had overall fewer bacteria (Figure 5a and d). For example, while the highest 16S rRNA gene count was observed in the Oa horizon of H* at $3.7e^{+10}$ copies/g dry weight (Figure 5a, 10-11 cm depth), the highest measured copy number from the NH profiles reached $7.4e^{+10}$ (plot 1), $9.7e^{+10}$ (plot 2), and $8.85e^{+10}$ (plot 3, Figure 5d) copies/g dry weight. All profiles (NH and H*) had the tendency of higher 16S rRNA gene copy numbers in upper horizons with the highest count being in the Oe horizon of plot 3 of the NH profile (0-3 cm depth).

The qPCR of the functional gene *pmoA*, quantifying methanotrophs, had contrasting distribution patterns. Here, the different primer combinations either resulted in roughly the same copy numbers in the NH and H* profiles (primer combination pmoA189-F/mb661-R), or in higher *pmoA* copy numbers in the H* profile (primer combination pmoA189-F/mb650-R). Generally, the primer combination pmoA189-F/mb650-R resulted in copy numbers/g dry weight about two orders of magnitude higher than the primer combination pmoA189-F/mb661-R. Still, both primer combinations resulted in similar patterns: the Oa horizon of the H* profile (10-11 cm depth) had the highest *pmoA* counts of all measured samples with a highest measurement of $7.1e^{+05}$ copies/g dry weight (pmoA189-F/mb661-R) and $2.5e^{+09}$ copies/g dry weight (pmoA189-F/mb650-R, Figure 5b), respectively. The NH profile, on the other hand, had its highest copy numbers in the Ahg horizon (15-29 cm depth) for the primer combination pmoA189-F/mb650-R with $2.9e^{+08}$ copies/g dry weight (Figure 5f). The primer combination pmoA189-F/mb661-R resulted in the much lower *pmoA* peak of $5.6e^{+05}$ copies/g dw in the lower Ahgf horizon (Figure 5e, 29-44 cm depth). Generally, the gene *pmoA* was only detected in the upper horizons of the H* profile, i.e. in the

https://doi.org/10.5194/egusphere-2026-3054
Preprint. Discussion started: 15 June 2026

O-horizons (0-11 cm depth) and the Ah@1 horizon (11-25 cm depth), while it was detected throughout most of the active layer of the NH profile, reaching down to its Ahgf horizon (29-44 cm depth).

The methyl coenzyme M reductase gene *mcrA*, an indicator for methanogenesis, was only found in plots 1 and 2 of the NH site, with its highest amount reaching up to $2.3e^{+07}$ copies/g dry weight in the Oa horizon (see Appendix B Table B1). However, all other *mcrA*-containing samples had much lower values, at or below $2.7e^{+05}$ copies per gram dry weight. It was not detected at all in the H* profile.

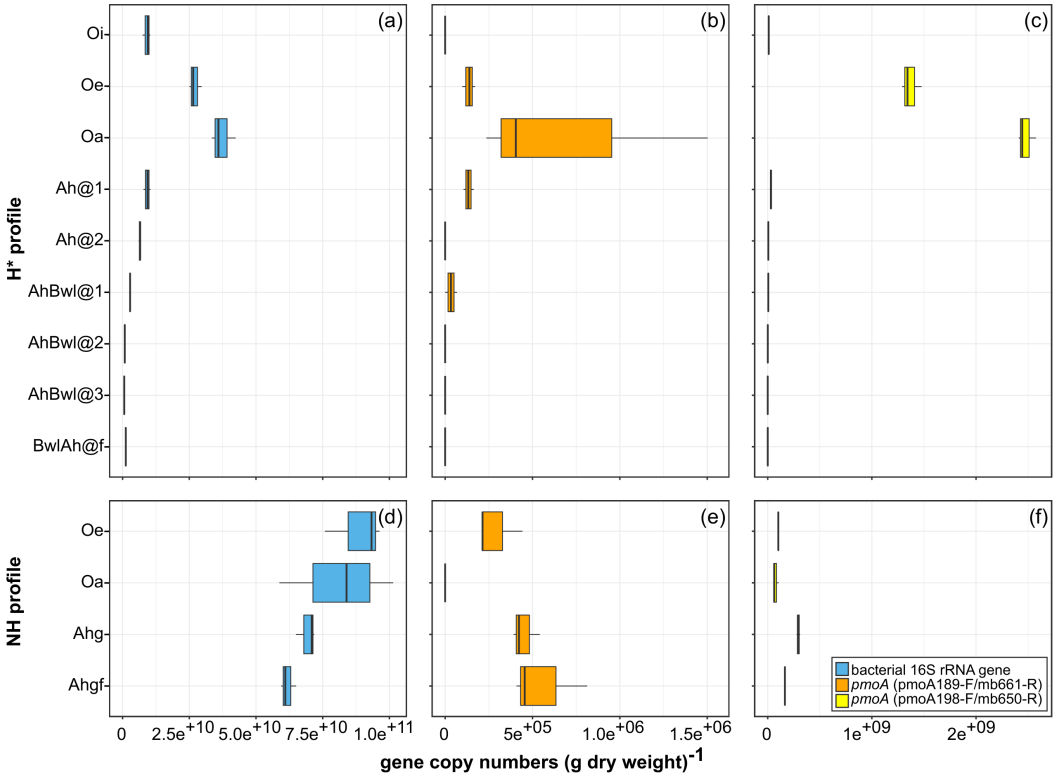

Figure 5: Quantitative PCR results on the bacterial 16S rRNA gene and particulate methane monooxygenase (*pmoA*) gene copy numbers. For H* profile, plot 3 (a, b and c) and the NH profile (d, e and f), gene copy numbers are calculated per g soil dry weight. The bacterial 16S rRNA gene is depicted in panels a and d, while *pmoA* copy numbers are shown derived from two different analyses: with the primer combination pmoA189-F/mb661-R (b and e) and the primer combination pmoA189-F/mb650-R (c and f). Extensive graphs of all plots and primer combinations can be viewed in the Supplement.

3.2.2 Community composition of methane oxidizers and methane producers

After processing and filtering the data, a total of 3,996 prokaryotic ASVs (a proxy for phylogenetic taxa) across a total of 13 samples (four samples along a depth gradient for NH and nine for H*) were identified. Of these, only 11 ASVs were identified as Archaea, with the remainder belonging to the domain of Bacteria. The alpha diversity (Shannon Diversity Index, calculated after filtering, but before removal of singletons and doubletons) was comparable between the NH and H* profile, with the values ranging from 5.49 (H*, Oa horizon) to 6.48 (NH, Ahgf horizon).

https://doi.org/10.5194/egusphere-2026-3054
Preprint. Discussion started: 15 June 2026

295 Four taxa belonging to aerobic methane-oxidizing bacteria were found in all samples (Figure 6). The obligate methanotroph *Methylobacter* was found in lower horizons of the NH soil profile (Figure 6b). The upper horizons of the H* profile mostly harbored the facultative methanotrophs *Methylocapsa* and *Methylocella*. The dominant methanotroph of the NH profile was the obligate methanotroph *Methylobacter* in lower soil horizons. Additionally, two families - Methylacidiphilaceae and Methyloligellaceae - were detected that have been reported to contain methanotrophs before (e.g. Vekeman et al., 2016,
300 Awala et al., 2023). It was not possible to confirm that methanotrophs belonging to this family were present in the analyzed samples, which is why they are only shown as potentially methanotroph-containing taxa. The H* profile had the highest relative abundance of confirmed methanotrophs in the relatively shallow Oe horizon (5-10 cm depth), reaching up to approximately 1.3 % of all reads (Figure 6a). The NH profile reached a maximum of approximately 0.8 % methanotrophs among all reads (Figure 6b) in the much deeper Ahg horizon (15-29 cm depth). Metabarcoding did reveal the presence of
305 methanogens. In particular, one ASV assigned to the methane-producing archaeal order Methanomassiliicoccales was detected in low relative abundance (below 0.1 % of all reads) in the horizons AhBwl@1, AhBwl@2, and BwlAh@f, i.e. 42 cm depth and below, of the H* profile.The metabarcoding results of the remaining NH replicates also showed consistently lower relative abundances of methanotrophs and specifically more facultative methanotrophs in lower soil horizons (see Appendix B Figure B4).

310

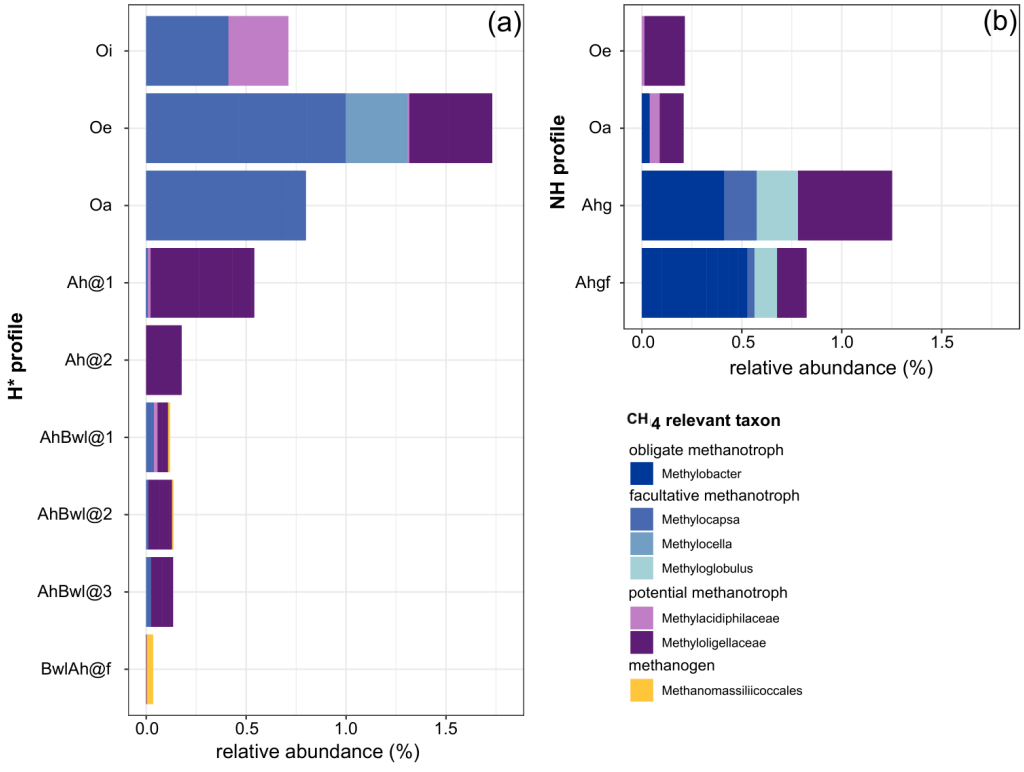

Figure 6: Relative abundance of potential methanotrophs and methanogens. Shown are methane-relevant prokaryotes found in the H* (a) and in NH (b). ASVs were filtered from mitochondria, eukaryotes and chloroplasts, as well as low
315 abundance ASVs before normalizing the samples to 100 % total.

https://doi.org/10.5194/egusphere-2026-3054
Preprint. Discussion started: 15 June 2026

3.3 Greenhouse Gas Flux Dynamics

Methane flux measurements showed distinct differences in greenhouse gas exchange dynamics among the three study sites H, IH, and NH. The H site consistently functioned as a net methane sink, exhibiting the highest mean uptake rate of -77 ± 74 µg CH_4 m^{-2} h^{-1} (n=44). The distribution of instantaneous fluxes was characterized by high variability and a distinct negative skew (Figure 7a). In contrast, the NH site functioned as a weaker sink, with a mean flux of -18 ± 10 µg CH_4 m^{-2} h^{-1} (n=68). The flux distribution for the NH site was narrower and clustered closer to zero compared to the H site. The IH site mean fluxes near the instrumental detection limit of 0.9 CH_4 µg m^{-2} h^{-1} (0.8 ± 0.28 µg CH_4 m^{-2} h^{-1}, n=44) fluctuating between negligible uptake and emission with no distinct directional trend. This resulted in cumulative budget trends over the measurement period that varied significantly across the study sites (Figure 7b). The H site displayed a linear accumulation of negative fluxes, resulting in a total seasonal uptake of -130 ± 8 mg CH_4 m^{-2}. The linearity of the cumulative curve indicates that uptake rates remained relatively constant throughout the measurement period, without a pronounced seasonal maximum or minimum. The NH site accumulated a total uptake of -31 ± 0.8 mg CH_4 m^{-2}, representing approximately 24 % of the sink strength observed at the H site. For the IH site, no distinct sink or source behavior was detectable.

Despite seasonal fluctuations in abiotic conditions, methane uptake rates in the H site appear barely influenced by standard meteorological drivers. Mean monthly soil temperatures at 10 cm depth followed a seasonal progression, rising from 3.9 °C in July to a maximum of 6.6 °C in August, before declining to 2.1 °C in September. This thermal variation did not correspond to a significant change in methane flux rates ($p > 0.05$, $n = 47$). Similarly, the deepening of the active layer, which reached a maximum thaw depth of 74 cm by late August, showed no significant linear relationship with the observed fluxes ($p > 0.05$, n=25). Neither a significant linear correlation was observed between instantaneous methane fluxes and air temperature and photosynthetically active radiation (PAR). Also, methane exchange in the NH site displayed also no dependence from seasonal environmental drivers. Although mean soil temperatures at 10 cm depth followed a typical seasonal trend, peaking at 4.0 °C in August before dropping to 1.0 °C in September, this thermal variation did not influence methane flux rates ($p > 0.05$, n=62). The development of the active layer was notably shallower than in H, reaching a maximum thaw depth of only 41 cm by late August.

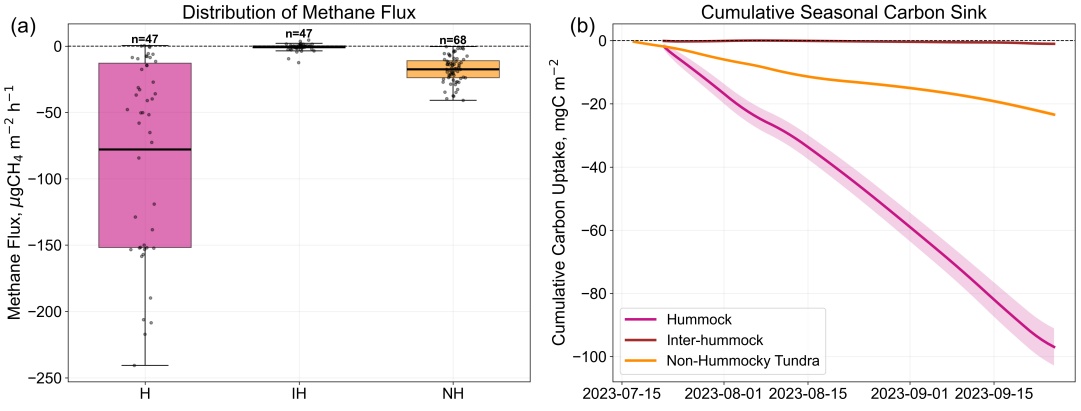

Figure 7: Methane flux dynamics (a) Methane flux measurements distribution for the hummock site (H, pink), the inter-hummock hollow (IH, brown) and the non-hummocky tundra (NH, orange) with horizontal lines indicating the hourly median methane flux (µg CH_4 m^{-2} h^{-1}). Individual field measurements are overlaid as black points, and the total sample size (*n*) is indicated above each plot. (b) Cumulative carbon sink strength over growing season (mg C m^{-2}), calculated by

https://doi.org/10.5194/egusphere-2026-3054
Preprint. Discussion started: 15 June 2026

integrating linearly interpolated daily mean fluxes measurement period. Shaded bands represent the cumulative propagated standard error of the mean (SEM).

4. Discussion

4.1 Micro-topographical regulation of spatial methane sink heterogeneity

While the release of CH_4 from thawing organic-rich permafrost has garnered significant attention, the compensatory potential of non-watersaturated cryosols of dry and moist tundra ecosystems to oxidize CH_4 still remains frequently underestimated in Arctic carbon budget assessments (Zhuang et al., 2013; Oh et al., 2020). The spatial distribution of CH_4 fluxes across our study area confirms that microtopography is an important regulator of methane sink strength in Arctic tundra (D'Imperio et al., 2017; Voigt et al., 2026). In our research area Kuup Ilua, we found strong differences in methane sink strengths between earth hummock tundra (Umbric Turbic Cryosol), which acted as robust methane sinks (-77 ± 74 µg CH_4 m^{-2} h^{-1}, n=44), compared to non-hummocky tundra (Mollic Cryosol; -18 ± 10 µg CH_4 m^{-2} h^{-1}, n=68). The inter-hummock depressions adjacent to the elevated hummocks (Skeletic Cryosol) IH fluctuated near the gas flux detection limit with no directional trend, and is thus considered negligible for the net methane budget of this specific landscape feature. The magnitude of uptake observed in the cryoturbated earth hummocks aligns well with values reported for other High Arctic mineral soils, such as the -92 µg CH_4 m^{-2} h^{-1}, reported across West Greenland and western Canadian Arctic (D'Imperio et al., 2023; Voigt et al., 2023). Weekly measurements between July and September 2023 reveal that the earth hummock sites accumulated a substantial growing season sink of -97 ± 6 mg C m^{-2}, placing them among the more active tundra landscape features of methane oxidation in the Arctic (Jørgensen et al., 2015; Voigt et al., 2026). In contrast, the non-hummocky tundra represented only ~24% of the hummock's growing season sink strength (-23 ± 0.6 mg C m^{-2}), supporting the hypothesis that mineral soils provide a widespread but variable background sink (Lau et al., 2015; D'Imperio et al., 2023).

We attribute this difference to the elevated microrelief of the hummock, where cryogenic uplift provides an elevated and well-aerated soil column (Trotsenko & Khmelenina, 2005), lowering the water table depth relative to the soil surface and exposing a larger volume of porous soil to atmospheric infiltration (Hermesdorf et al., 2022; Lee et al., 2023). This structural elevation increases the vertical effective diffusivity of the soil column, allowing atmospheric methane to penetrate deep into the horizons where high-affinity methanotrophic communities are concentrated (Knoblauch et al., 2008; D'Imperio et al., 2023). Further, the association of strong uptake with shrub-covered hummocks aligns with findings that vascular plant cover, particularly dwarf shrubs like *Dryas* and *Salix*, facilitates methane oxidation (Lee et al., 2023; Voigt et al., 2026). We propose that these shrubs restructure the soil through extensive root systems that create wider pore spaces, thereby enhancing gas transport (Wilcox et al., 2019; Voigt et al., 2023). Furthermore, the transpiration activity of shrubs actively lowers the water table within the hummock core, expanding the aerated vadose zone available for microbial activity (Lee et al., 2023, Voigt et al., 2026). This creates a stable hydrological regime where the micro-topography allows for rapid runoff during heavy rainfall, preventing the saturation that inhibits aerobic oxidation (D'Imperio et al., 2017, Hermesdorf et al., 2022).
Conversely, the thick moss carpet (*Tomentypnum*) observed in the non-hummocky tundra appears to act as a dual physical and thermal barrier for CH_4 uptake (Gornall et al., 2007). These moss carpets have a strong insulating effect that can delay active layer thaw and maintains the underlying soil in a colder, wetter state, which limits the metabolic rates of methanotrophs (Gornall et al., 2007; D'Imperio et al., 2017). Furthermore, the dense moss structure likely inhibits the intake of atmospheric methane by reducing surface diffusivity (Knoblauch et al., 2008; Hermesdorf et al., 2022). The almost complete lack of uptake in the saturated inter-hummock depressions further supports a "lid effect", where water-logging

https://doi.org/10.5194/egusphere-2026-3054
Preprint. Discussion started: 15 June 2026

prevents atmospheric interaction and limits the colonization of high-affinity methanotrophic organisms (Knoblauch et al., 2008; Martineau et al., 2014).

4.2 Influence of soil pH and microbial community structure on methane uptake potential

On a global scale, atmospheric CH_4 levels are primarily regulated by tropospheric oxidation, yet the terrestrial soil sink remains the second-largest removal pathway, accounting for approximately 5–10 % of the total CH_4 budget (Conrad, 2009; Saunois et al., 2020; Folberth et al., 2025). However, the strength of this biotic sink is not a static global constant; rather, it is highly sensitive to localized soil properties, which govern the interaction between the atmosphere and the soil microbiome (Oh et al., 2020; Lee et al., 2023). In Arctic tundra ecosystems, this sensitivity is particularly pronounced due to extreme landscape heterogeneity. While broad-scale models often rely on regional thermal drivers, such as air temperature, to predict fluxes, these variables frequently fail to explain the dramatic variations in CH_4 exchange observed across small spatial scales (Knoblauch et al., 2008; Zhuang et al., 2013).

The difference in CH_4 uptake capacity between the hummocks and non-hummocky tundra that we observed is likely a result of cryogenic microtopography. The significant pH disparity between the hummock and the non-hummocky tundra is primarily driven by the decoupling from lateral flow of groundwater or soil interflow water along the slopes facilitated by the elevated microrelief of the hummocks. The elevation of the hummock crest above the mean water table reduces the influence of groundwater, which otherwise provides a replenishing effect against acidification through the lateral or upward flux of minerogenic base-rich water (Tarnocai and Zoltai, 1978). In contrast, the inter-hummock hollows remain at near-neutral pH because they stay saturated longer and maintain closer contact with minerogenic soil or ground water or meltwater from thawing ground ice containing dissolved cations (Peplau et al., 2025). In the well-drained hummock crest, the accumulation of organic matter leads to the active production of organic acids during decomposition. This acidity is further reinforced by the leaching of base cations, which are washed out of the aerated upper horizon by rainfall, resulting in a localized drop in pH to approximately ~4.5. However, these features do not reach full ombrotrophication, the state of receiving nutrients solely from rain, because the organic layer remains thin and cryoturbation constantly mixes mineral soil back into the organic horizon, counteracting total isolation of water and nutrient flows from the subsoil. In contrast, the non-hummock tundra maintains higher moisture with higher lateral water throughflow and retains a more moderate pH of ~6.0.

Further, in our study, the *pmoA* gene (targeting a subunit of the particulate methane monooxygenase, pMMO) was significantly more abundant in the upper horizons of the hummock, despite the non-hummocky tundra having a higher overall microbial biomass (measured via 16S rRNA gene copies). This indicates that the hummock top soils are an optimized habitat for methanotrophs, whereas the non-hummocky tundra hosts a larger, but more generalist, microbial community. This disparity aligns with findings that coarser, better-drained soils facilitate aerobic methane oxidizers necessary for CH_4 oxidation (Dutaur & Verchot, 2007; Knoblauch et al., 2008, Voigt et al., 2026). The resulting pH gradient acts as the primary driver of microbial community assembly, a phenomenon defined as "pH-based ecological coherence" (Zhao et al., 2020; Yao et al., 2023).

Without sequencing of the *pmoA* gene, definitive methane affinities of the found methanotrophs remains difficult. However, the metabarcoding-based taxonomic identification, combined with the environmental parameters and gas fluxes, strongly suggest the oxidation strategies of the detected methanotrophs. *Methylocapsa*, the dominating methanotrophic genus found in the hummock, is reported to contain several high-affinity methanotrophic species (Tveit et al., 2019). The second most dominant methanotroph in the hummock is *Methylocella*, which is often isolated from high CH_4-environments (Dedysh et

https://doi.org/10.5194/egusphere-2026-3054
Preprint. Discussion started: 15 June 2026

al., 2005; Haque et al., 2019). However, due to its versatility in carbon sources, it is most likely a low- to moderate-affinity methanotroph. The Type-IIB methanotrophs *Methylocapsa* and *Methylocella* are often obligate acidophiles whose enzymatic systems are specifically optimized for sub-atmospheric CH_4 concentrations of approximately 1.9 ppm (Dedysh et al., 1998; Tveit et al., 2019). To survive in acidic, nutrient-poor hummocks, the methanotrophic community utilizes significant metabolic plasticity. High-affinity methanotrophs, including *Methylocapsa*, supplement their energy by oxidizing atmospheric hydrogen (H_2) and carbon monoxide (CO) (Tveit et al., 2019; Bay et al., 2021). Furthermore, their ability to fix dinitrogen (N_2) allows them to bypass the nitrogen limitations typical of leached acidic soils (Tveit et al., 2019; Voigt et al., 2026). Furthermore, *Methylocella* was not targeted by the qPCR analyses carried out in this study targeting the *pmoA* gene, because it exclusively utilizes the soluble methane monooxygenase (sMMO) for methane oxidation (Fenibo et al., 2023). This is why we conclude that the total genetic potential for methane oxidation in this profile was very likely underestimated with the qPCR approach.

The most dominant methanotroph of the non-hummocky tundra is *Methylobacter*, which is a low- to medium-affinity methanotroph (Smith et al., 2018). *Methylobacter* is reported to be an obligate methanotroph, who is typical of more moderate pH conditions (Smith et al., 2018), can likely use either sMMO or pMMO for methane oxidation, but certainly has the *pmoA* gene (Knief, 2015). The method bias for the non-hummocky tundra was therefore likely smaller than for the hummock. Former findings of *Methyloglobulus*, the second-most-dominant methanotroph of the non-hummocky tundra, show no clear kinetic data for CH_4 oxidation. However, its limited choice of electron donors (methane and methanol) and initial cultivation from a high-CH_4 environment (Deutzmann et al., 2014) suggest a tendency towards low-affinity methanotrophy. Martineau et al. (2014) further segregated methanotrophic communities by pH, reporting high-affinity methanotrophs in acidic soils and low-affinity methanotrophs in neutral soils, which is in line with our findings. The hummock is therefore a habitat for high-affinity and atmospheric methanotrophs in contrast to the non-hummocky tundra, which mostly contains low- to medium-affinity methanotrophs. This suggests that the methanotrophs in the non-hummocky tundra presumably offset methane from lower, anoxic soil horizons, while the hummock was able to oxidize atmospheric methane.

Interestingly, we detected sequences of the order Methanomassiliicoccales in the lower hummock horizons in very low relative abundances, yet no *mcrA* gene was detected via qPCR. It is likely that the detected member of the Methanomassiliicoccales was so low in abundance that the qPCR simply failed to detect. Overall, our data indicate that methanogenesis is negligible in hummocks.

4.3 Implications on the Arctic Carbon Budget

The integration of our findings into the broader Arctic carbon budget highlights the critical importance of microtopography for upscaling. Zhuang et al. (2013) and Oh et al. (2020) argue that process-based models frequently overestimate net methane emissions because they fail to adequately parameterize the sink strength of dry, mineral soils. Our data highlight a significant scaling error inherent in landscape homogenization. If a regional model treats the tundra as a uniform pixel based on the non-hummocky tundra average, it would underestimate the potential methane sink capacity by approximately 75 % relative to the actual contribution of earth hummocks. Conversely, if the landscape is classified broadly as "wet tundra" based on the characteristics of inter-hummock hollows, the persistent sink function of these mineral features is ignored entirely in favor of assumed net emissions. This supports the claim by Martineau et al. (2014) and Voigt et al. (2026) that accurate mapping of microbial community distribution and their associated soil classification is a prerequisite for accurate global budgets.

https://doi.org/10.5194/egusphere-2026-3054
Preprint. Discussion started: 15 June 2026

The ongoing "greening" of the Arctic, characterized by the expansion of deciduous shrubs, may introduce a significant negative feedback mechanism into the regional carbon cycle (Wilcox et al., 2019; Voigt et al., 2026). We observed the highest methane uptake rates in hummocks dominated by dwarf shrubs like *Dryas* and *Salix*, whose root systems likely facilitate gas transport and active soil aeration (Lee et al., 2023; Voigt et al., 2026). If continued warming promotes shrub expansion, the resulting increase in evapotranspiration and soil structural complexity could broaden the area extent of these high-affinity methane sinks (Wilcox et al., 2019; Lee et al., 2023). This suggests that as the climate warms, the capacity of the soil to take up atmospheric methane may increase.

However, the stability of this Arctic methane sink is critically threatened by geomorphological degradation driven by accelerating permafrost thaw (Rößger et al., 2022). The warming induced ground subsidence, could lead to the rapid collapse of elevated, dry hummocks into water-saturated depressions. Our results indicate that the conversion of an earth hummock to an inter-hummock depression does not simply result in a marginal reduction of sink strength, but rather a total omission of methane uptake. In this scenario, the loss of specialized acidic, well aerated niches and the onset of anaerobic conditions would weaken the region's ability to bind atmospheric methane. Therefore, the future trajectory of the Arctic methane balance depends less on uniform temperature responses and more on the structural evolution of the frost-patterned landscape. Accurate predictions of the Arctic's role in the global methane cycle must, therefore, account for the delicate balance between the expansion of shrub-driven sinks and the loss of these niches through warming-induced permafrost degradation and subsidence.

5. Conclusion

Our study demonstrates that methane CH_4 exchange in the Arctic tundra is strongly regulated by cryogenic microtopography affecting soil chemistry and microbial community assembly. Our measurements reveal a strong divergence in methane sink capacity of Arctic landscape features: while inter-hummock hollows remain biogeochemically inert, cryoturbated earth hummocks can function as substantial atmospheric methane sinks, especially when compared to non-hummocky tundra. The mechanism driving this high-intensity methane sink is the cryopedogenesis of the earth hummock. Cryogenic uplift creates an elevated micro-environment characterized by deep drainage and an expanded vadose zone, physically isolating the soil column from the surrounding water table and lateral water flows. This structural separation facilitates the leaching of base cations and the relative accumulation of organic acids from shrub litter, leading to significant localized soil acidification (pH ~4.5). We identify this acidic, oligotrophic niche as the primary selective filter for the soil microbiome, inhabiting specialized high-affinity methanotrophs. Particularly, the genus *Methylocapsa* dominates these acidic upper organic soil horizons, utilizing particulate methane monooxygenase (pMMO) to enduringly metabolize methane at trace atmospheric concentrations. Further, our data also reveals a decoupling of methane uptake rates from seasonal soil warming. This indicates that in these well-drained mineral soils, the metabolic activity of the methanotrophic community is constrained by substrate availability and physical transport mechanisms rather than standard thermal kinetics. Ultimately, this study identifies cryoturbated earth hummocks as critical, micro-topography-driven, highly effective methane sinks whose functional capacity is determined by the synergy of physical aeration, localized acidification, and taxonomic specialization.

https://doi.org/10.5194/egusphere-2026-3054
Preprint. Discussion started: 15 June 2026

Author contributions

Selina Undeutsch: Writing (original draft preparation), Visualization, Validation, Methodology, Formal analysis, Data curation, Conceptualization. **Claudia S. Bruhn:** Writing (original draft preparation), Visualization, Validation, Methodology, Formal analysis, Data curation, Conceptualization. **Tino Peplau:** Validation, Investigation, Formal analysis. **Birgit Grabellus:** Investigation, Formal analysis. **Sina Plettemeier:** Investigation, Formal analysis. **Susanne Liebner:** Supervision, Resources, Investigation, Funding acquisition, Writing (review and editing). **Lars Kutzbach:** Supervision, Resources, Investigation, Funding acquisition, Formal analysis, Writing (review and editing), Conceptualization.

These authors contributed equally to this work: **Selina Undeutsch** and **Claudia S. Bruhn**.

Funding and Acknowledgements

The samples were taken and processed under Genetic Resource License G24-133 issued by the Greenlandic government. The presented work was supported by the German Federal Ministry of Education and research under the project MOMENT (grant numbers 03F0931A, 03F0931C, and 03F0931E). The work was further supported under POF IV topic 5 of the Helmholtz Association of Research Centers. Thank you to Alexander Bartholomäus for the processing of the raw bioinformatics data. Furthermore, our thanks go to Anke Saborowski for her support in the molecular laboratory. Additionally, we want to thank Bo Elberling, Kjeld Akaaraq Mølgaard and the rest of the Arctic Station staff for their support during the field campaigns.

Declaration of competing interest

The authors declare that they have no competing interests that could have appeared to influence the work reported in this paper.

Copernicus Disclaimer

Copernicus Publications remains neutral with regard to jurisdictional claims made in the text, published maps, institutional affiliations, or any other geographical representation in this paper. While Copernicus Publications makes every effort to include appropriate place names, the final responsibility lies with the authors. Views expressed in the text are those of the authors and do not necessarily reflect the views of the publisher.

Data availability

Supplementary data to “Earth hummock soils as hot-spot of atmospheric methane uptake in Arctic tundra: a case study from Qeqertarsuaq, West Greenland” (Original data) is made available in the supplements.

https://doi.org/10.5194/egusphere-2026-3054
Preprint. Discussion started: 15 June 2026

References

Angel, R., Claus, P., and Conrad, R.: Methanogenic archaea are globally ubiquitous in aerated soils and become active under wet anoxic conditions, ISME J., 6, 847–862, https://doi.org/10.1038/ismej.2011.141, 2012.Bartsch, A., Efimova, A., Widhalm, B., Muri, X., von Baeckmann, C., Bergstedt, H., Ermokhina, K., Hugelius, G., Heim, B., and Leibman, M.: Circumarctic land cover diversity considering wetness gradients, Hydrol. Earth Syst. Sci., 28, 2421–2481, https://doi.org/10.5194/hess-28-2421-2024, 2024.

Bay, S. K., Dong, X., Bradley, J. A., Leung, P. M., Grinter, R., Jirapanjawat, T., Arndt, S. K., Cook, P. L. M., LaRowe, Nauer, P. A., Chiri, E., and Greening, C..: Trace gas oxidizers are widespread and active members of soil microbial communities, Nat. Microbiol., 6, 246–256, https://doi.org/10.1038/s41564-020-00811-w, 2021.

Bourne, D. G., McDonald, I. R., and Murrell, J. C.: Comparison of *pmoA* PCR primer sets as tools for investigating methanotroph diversity in three Danish soils, *Appl. Environ. Microbiol.*, **67**, 3802–3809, https://doi.org/10.1128/AEM.67.9.3802-3809.2001, 2001.

Burn, C. R.: The active layer: two contrasting definitions, Permafrost Periglac. Process., 9, 411–416, https://doi.org/10.1002/(SICI)1099-1530(199810/12)9:4<411::AID-PPP293>3.0.CO;2-6, 1998.

Callahan, B. J., McMurdie, P. J., Rosen, M. J., Han, A. W., Johnson, A. J. A. and Holmes, S. P.: DADA2: High-resolution sample inference from Illumina amplicon data, Nat. Methods, 13, 581–583, https://doi.org/10.1038/nmeth.3869, 2016.

Caporaso, J. G., Lauber, C. L., Walters, W. A., Berg-Lyons, D., Lozupone, C. A., Turnbaugh, P. J., Fierer, N., and Knight, R.: Global patterns of 16S rRNA diversity at a depth of millions of sequences per sample, *Proc. Natl. Acad. Sci. U.S.A.*, **108**(Suppl. 1), 4516–4522, https://doi.org/10.1073/pnas.1000080107, 2011.

Chadburn, S. E., Burke, E. J., Cox, P. M., Friedlingstein, P., Hugelius, G., and Westermann, S.: An observation-based constraint on permafrost loss as a function of global warming, Nature Clim. Change, 7, 340–344, https://doi.org/10.1038/nclimate3262, 2017.

Conrad, R.: The global methane cycle: recent advances in understanding the microbial processes involved, Environ. Microbiol. Rep., 1, 285–292, https://doi.org/10.1111/j.1758-2229.2009.00038.x, 2009.

Dedysh, S. N., Knief, C., and Dunfield, P. F.: *Methylocella* species are facultatively methanotrophic, J. Bacteriol., 187, 4665–4670, https://doi.org/10.1128/JB.187.13.4665-4670.2005, 2005.

Dedysh, S. N., Panikov, N. S., Liesack, W., Großkopf, R., Zhou, J., and Tiedje, J. M.: Isolation of acidophilic methane-oxidizing bacteria from northern peat wetlands, Science, 282, 281–284, https://doi.org/10.1126/science.282.5387.281, 1998.

Costello, A. M. and Lidstrom, M. E.: Molecular characterization of functional and phylogenetic genes from natural populations of methanotrophs in lake sediments, *Appl. Environ. Microbiol.*, **65**, 5066–5074, https://doi.org/10.1128/AEM.65.11.5066-5074.1999, 1999.

Deutzmann, J. S., Hoppert, M., and Schink, B.: Characterization and phylogeny of a novel methanotroph, *Methyloglobulus* morosus gen. nov., spec. nov., Syst. Appl. Microbiol., 37, 165–169, https://doi.org/10.1016/j.syapm.2014.02.001, 2014.

Dutaur, L. and Verchot, L. V.: A global inventory of the soil CH4 sink, Global Biogeochem. Cy., 21, GB4005, https://doi.org/10.1029/2006GB002734, 2007.

D'Imperio, L., Li, B., Tiedje, J. M., Jiang, Y., Christensen, T. R., Kramshøj, M., Nielsen, C. S., Priemé, A., Westergaard-Nielsen, A., and Elberling, B.: Spatial controls of methane uptake in upland soils across climatic and geological regions in Greenland, Commun. Earth Environ., 4, 461, https://doi.org/10.1038/s43247-023-01143-3, 2023.

D'Imperio, L., Nielsen, C. S., Westergaard-Nielsen, A., Michelsen, A., and Elberling, B.: Methane oxidation in contrasting soil types: Responses to experimental warming with implication for landscape-integrated CH4 budget, Global Change Biol., 23, 966–976, https://doi.org/10.1111/gcb.13400, 2017.

https://doi.org/10.5194/egusphere-2026-3054
Preprint. Discussion started: 15 June 2026

Fenibo, E. O., Selvarajan, R., Wang, H., Wang, Y., and Abia, A. L. K.: Untapped talents: insight into the ecological significance of methanotrophs and its prospects, Sci. Total Environ., 903, 166145, https://doi.org/10.1016/j.scitotenv.2023.166145, 2023.

Fetzer, S., Bak, F., and Conrad, R.: Sensitivity of methanogenic bacteria from paddy soil to oxygen and desiccation, FEMS Microbiol. Ecol., 12, 107–115, https://doi.org/10.1111/j.1574-6941.1993.tb00022.x, 1993.

Folberth, G. A., Jones, C. D., O'Connor, F. M., Rumbold, S. T., Gedney, N., and Robertson, E.: Drivers of persistent changes in the global methane cycle under aggressive mitigation action, npj Clim. Atmos. Sci., 8, 136, https://doi.org/10.1038/s41612-024-00867-z, 2025.

Fox, J. and Weisberg, S.: An R Companion to Applied Regression, 3rd edn., Sage, Thousand Oaks, CA, USA, 2019.

French, H. M.: The periglacial environment, John Wiley & Sons, Hoboken, NJ, https://doi.org/10.1002/9781119132820, 2018.

Frost, G. V., Epstein, H. E., Walker, D. A., Matyshak, G., and Ermokhina, K.: Patterned-ground facilitates shrub expansion in Low Arctic tundra, Environ. Res. Lett., 8, 015035, https://doi.org/10.1088/1748-9326/8/1/015035, 2013.

Geoffroy, L., Gelard, J. P., Lepvrier, C., and Olivier, P.: The coastal flexure of Disko (West Greenland), onshore expression of the 'oblique reflectors', J. Geol. Soc., 155, 463–473, https://doi.org/10.1144/gsjgs.155.3.0463, 1998.

Gillespie, A. W., Sanei, H., Diochon, A., Ellert, B. H., Regier, T. Z., Chevrier, D., Dynes, J. J., Tarnocai, C., and Gregorich, E. G.: Perennially and annually frozen soil carbon differ in their susceptibility to decomposition: Analysis of Subarctic earth hummocks by bioassay, XANES and pyrolysis, Soil Biol. Biochem., 68, 106–116, https://doi.org/10.1016/j.soilbio.2013.09.021, 2014.

Gornall, J. L., Jónsdóttir, I. S., Woodin, S. J., and Van der Wal, R.: Arctic mosses govern below-ground environment and ecosystem processes, Oecologia, 153, 931–941, https://doi.org/10.1007/s00442-007-0785-0, 2007.

Gottuk, J., Stuenzi, S. M., Runge, A., and Boike, J.: Assessing midsummer snow-free land surface albedo variability across multiple Arctic sites using the Harmonized Landsat and Sentinel-2 product, Sci. Remote Sens., 12, 100283, https://doi.org/10.1016/j.srs.2025.100283, 2025.

Haque, M. F. U., Crombie, A. T., and Murrell, J. C.: Novel facultative Methylocella strains are active methane consumers at terrestrial natural gas seeps, Microbiome, 7, 134, https://doi.org/10.1186/s40168-019-0741-3, 2019.

Hermesdorf, L., Elberling, B., D'Imperio, L., Xu, W., Lambæk, A., and Ambus, P. L.: Effects of fire on CO_2, CH_4, and N_2O exchange in a well-drained Arctic heath ecosystem, Global Change Biol., 28, 4882–4899, https://doi.org/10.1111/gcb.16222, 2022.

Hermesdorf, L., Liu, Y., Michelsen, A., Westergaard-Nielsen, A., Mortensen, L. H., Jepsen, M. S., Hollesen, J., and Elberling, B.: Long-term changes in the daytime growing season carbon dioxide exchange following increased temperature and snow cover in arctic tundra, Global Change Biol., 30, e17087, https://doi.org/10.1111/gcb.17087, 2024.

Holl, D., Kutzbach, L., and Eckhardt, T.: AG Kutzbach chamberflux, [data set], https://doi.org/10.25592/uhhfdm.18485, 2026.

Hollesen, J., Buchwal, A., Rachlewicz, G., Hansen, B. U., Hansen, M. O., Stecher, O., and Elberling, B.: Winter warming as an important co-driver for Betula nana growth in western Greenland during the past century, Global Change Biol., 21, 2410–2423, https://doi.org/10.1111/gcb.12913, 2015.

Hugelius, G., Strauss, J., Zubrzycki, S., Harden, J. W., Schuur, E. A. G., Ping, C.-L., Schirrmeister, L., Grosse, G., Michaelson, G. J., Koven, C. D., O'Donnell, J. A., Elberling, B., Mishra, U., Camill, P., Yu, Z., Palmtag, J., and Kuhry, P.: Estimated stocks of circumpolar permafrost carbon with quantified uncertainty ranges and identified data gaps, Biogeosciences, 11, 6573–6593, https://doi.org/10.5194/bg-11-6573-2014, 2014.

Jørgensen, C. J., Johansen, K. L. M., Westergaard-Nielsen, A., and Elberling, B.: Net regional methane sink in High Arctic soils of northeast Greenland, Nat. Geosci., 8, 20–23, https://doi.org/10.1038/ngeo2305, 2015.

https://doi.org/10.5194/egusphere-2026-3054
Preprint. Discussion started: 15 June 2026

Jørgensen, C. J., Mariager, T. S., and Christiansen, J. R.: Spatial variation of net methane uptake in Arctic and subarctic drylands of Canada and Greenland, Geoderma, 443, 116815, https://doi.org/10.1016/j.geoderma.2024.116815, 2024.

Kaiser, C., Meyer, H., Biasi, C., Rusalimova, O., Barsukov, P., and Richter, A.: Conservation of soil organic matter through cryoturbation in Arctic soils in Siberia, J. Geophys. Res., 112, G02017, https://doi.org/10.1029/2006JG000258, 2007.

Kelley, S. E., Briner, J. P., and Young, N. E.: Rapid ice retreat in Disko Bugt supported by 10Be dating of the last recession of the western Greenland Ice Sheet, Quat. Sci. Rev., 82, 13–22, https://doi.org/10.1016/j.quascirev.2013.09.018, 2013.

Knief, C.: Diversity and habitat preferences of cultivated and uncultivated aerobic methanotrophic bacteria evaluated based on *pmoA* as molecular marker, Front. Microbiol., 6, 1346, https://doi.org/10.3389/fmicb.2015.01346, 2015.

Knoblauch, C., Zimmermann, U., Blumenberg, M., Michaelis, W., and Pfeiffer, E.-M.: Methane turnover and temperature response of methane-oxidizing bacteria in permafrost-affected soils of northeast Siberia, Soil Biol. Biochem., 40, 3004–3013, https://doi.org/10.1016/j.soilbio.2008.08.020, 2008.

Kokelj, S. V., Burn, C. R., and Tarnocai, C.: The structure and dynamics of earth hummocks in the subarctic forest near Inuvik, Northwest Territories, Canada, Arctic Antarctic Alpine Res., 39, 99–109, https://doi.org/10.1657/1523-0430(2007)39[99:TSADOE]2.0.CO;2, 2007.

Koven, C., Friedlingstein, P., Ciais, P., Khvorostyanov, D., Krinner, G., and Tarnocai, C.: On the formation of high-latitude soil carbon stocks: Effects of cryoturbation and insulation by organic matter in a land surface model, Geophys. Res. Lett., 36, L21401, https://doi.org/10.1029/2009GL040150, 2009.

Lau, M. C. Y., Stackhouse, B. T., Layton, A. C., Chauhan, A., Vishnivetskaya, T. A., Chourey, K., Ronholm, J., Mykytczuk, N. C. S., Bennett, P. C., Lamarche-Gagnon, G., Burton, N., Pollard, W. H., Omelon, C. R., Medvigy, D., Hettich, R. L., Pfiffner, S. M., Whyte, L. G., and Onstott, T. C.: An active atmospheric methane sink in high Arctic mineral cryosols, ISME J., 9, 1880–1891, https://doi.org/10.1038/ismej.2015.13, 2015.

Lee, J., Yun, J., Yang, Y., Jung, J. Y., Lee, Y. K., Yuan, J., Park, H., and Kang, H.: Attenuation of methane oxidation by nitrogen availability in arctic tundra soils, Environ. Sci. Technol., 57, 2647–2659, https://doi.org/10.1021/acs.est.2c05228, 2023.

Lundqvist, J.: Patterned ground and related frost phenomena in Sweden, Sveriges Geologiska Undersökning, Ser. C, Nr. 583, Årsbok 55, No. 7, 1–101, 1962.

Mackay, J. R.: The origin of hummocks, western Arctic coast, Canada, Can. J. Earth Sci., 17, 996–1006, https://doi.org/10.1139/e80-100, 1980.

Martin, M.: Cutadapt removes adapter sequences from high-throughput sequencing reads, EMBnet.journal, 17, 10–12, https://doi.org/10.14806/ej.17.1.200, 2011

Martineau, C., Pan, Y., Bodrossy, L., Yergeau, E., Whyte, L. G., and Greer, C. W.: Atmospheric methane oxidizers are present and active in Canadian high Arctic soils, FEMS Microbiol. Ecol., 89, 257–269, https://doi.org/10.1111/1574-6941.12287, 2014.

McMurdie, P. J. and Holmes, S.: phyloseq: an R package for reproducible interactive analysis and graphics of microbiome census data, PLoS One, 8, e61217, https://doi.org/10.1371/journal.pone.0061217, 2013.

Murase, J., Sugimoto, A., Shingubara, R., Liang, M., Morozumi, T., Takano, S., and Maximov, T. C.: Methane oxidation potential of the Arctic wetland soils of a taiga–tundra ecotone in northeastern Siberia, *Soil Sci. Plant Nutr.*, **66**, 645–652, https://doi.org/10.1080/00380768.2020.1786343, 2020.

Muyzer, G., de Waal, E. C., and Uitterlinden, A. G.: Profiling of complex microbial populations by denaturing gradient gel electrophoresis analysis of polymerase chain reaction-amplified genes coding for 16S rRNA, *Appl. Environ. Microbiol.*, **59**, 695–700, https://doi.org/10.1128/AEM.59.3.695-700.1993, 1993.

https://doi.org/10.5194/egusphere-2026-3054
Preprint. Discussion started: 15 June 2026

Oh, Y., Zhuang, Q., Liu, L., Welp, L. R., Lau, M. C. Y., Onstott, T. C., Medvigy, D., Bruhwiler, L., Dlugokencky, E. J., Tans, P. P., and Miller, C. E.: Reduced net methane emissions due to microbial methane oxidation in a warmer Arctic, Nat. Clim. Change, 10, 317–321, https://doi.org/10.1038/s41558-020-0734-z, 2020.

Oksanen, J., Simpson, G., Blanchet, F., Kindt, R., Legendre, P., Minchin, P., O'Hara, R., Solymos, P., Stevens, M., Szoecs, E., Wagner, H., Bedward, M., Bolker, B., Borcard, D., Carvalho, G., De Cáceres, M., Durand, S., Evangelista, H., Hannigan, G., Hill, M., Lahti, L., Martino, C., Ouellette, M., Ribeiro Cunha, E., Smith, T., Stier, A., Ter Braak, C., and Weedon, J.: vegan: Community Ecology Package, R package version 2.8-0, https://vegandevs.github.io/vegan/, 2026.

Park, H., Gubin, S. V., Fedorov, A. N., and Kim, Y.: A biogeochemical study of greenhouse gas formation from two ice complexes of Batagay Megaslump, East Siberia, Permafrost Periglac. Process., 35, 437–449, https://doi.org/10.1002/ppp.2234, 2024.

Peplau, T., Liebmann, P., Fiencke, C., Undeutsch, S., Knoblauch, C., Dultz, S., Hildebrandt, A., Kutzbach, L., Elberling, B., Schnee, L. S., Melchert, J. O., Rethemeyer, J., Mikutta, C., and Guggenberger, G.: Soil development, mineralogy and organic matter stocks in a West Greenlandic tundra landscape, Catena, 260, 109436, https://doi.org/10.1016/j.catena.2025.109436, 2025.

Peterson, R. A. and Krantz, W. B.: A mechanism for differential frost heave and its implications for patterned-ground formation, J. Glaciol., 49, 69–80, https://doi.org/10.3189/172756503781830854, 2003.

Peterson, R. A. and Krantz, W. B.: Differential frost heave model for patterned ground formation: Corroboration with observations along a North American arctic transect, J. Geophys. Res.-Biogeo., 113, G03S04, https://doi.org/10.1029/2007JG000559, 2008.

Ping, C. L., Jastrow, J. D., Jorgenson, M. T., Michaelson, G. J., and Shur, Y. L.: Permafrost soils and carbon cycling, SOIL, 1, 147–171, https://doi.org/10.5194/soil-1-147-2015, 2015.

Posit team: RStudio: integrated development environment for R, version 2024.09.1+394, https://dailies.rstudio.com/version/2024.09.1+394, 2024.

Quast, C., Pruesse, E., Yilmaz, P., Gerken, J., Schweer, T., Yarza, P., Peplies, J. and Glöckner, F. O.: The SILVA ribosomal RNA gene database project: improved data processing and web-based tools, Nucleic Acids Res., 41, D590–D596, https://doi.org/10.1093/nar/gks1219, 2013.

R Core Team: R: A language and environment for statistical computing, R Foundation for Statistical Computing, Vienna, Austria, https://www.R-project.org/, 2024.

Rantanen, M., Karpechko, A. Y., Lipponen, A., Nordling, K., Hyvärinen, O., Ruosteenoja, K., Vihma, T., and Laaksonen, A.: The Arctic has warmed nearly four times faster than the globe since 1979, Commun. Earth Environ., 3, 168, https://doi.org/10.1038/s43247-022-00498-3, 2022.

Rößger, N., Sachs, T., Wille, C., Boike, J., Vesala, T., and Kutzbach, L.: Seasonal increase of methane emissions linked to warming in Siberian tundra, Nat. Clim. Change, 12, 1031–1036, https://doi.org/10.1038/s41558-022-01512-4, 2022.

Ruiz-Fernández, J., Oliva, M., Otero, X. L., and García-Hernández, C.: Morphometric and sedimentological characteristics of Late Holocene earth hummocks in the Zackenberg Valley (NE Greenland), Sci. Total Environ., 737, 140281, https://doi.org/10.1016/j.scitotenv.2020.140281, 2020.

Saunois, M., Stavert, A. R., Poulter, B., Bousquet, P., Canadell, J. G., Jackson, R. B., Raymond, P. A., Dlugokencky, E. J., Houweling, S., Patra, P. K., Ciais, P., Arora, V. K., Bastviken, D., Bergamaschi, P., Blake, D. R., Brailsford, G., Bruhwiler, L., Carlson, K. M., Carrol, M., Castaldi, S., Chandra, N., Crevoisier, C., Crill, P. M., Covey, K., Curry, C. L., Etiope, G., Frankenberg, C., Gedney, N., Hegglin, M. I., Höglund-Isaksson, L., Hugelius, G., Ishizawa, M., Ito, A., Janssens-Maenhout, G., Jensen, K. M., Joos, F., Kleinen, T., Krummel, P. B., Langenfelds, R. L., Laruelle, G. G., Liu, L., Machida, T., Maksyutov, S., McDonald, K. C., McNorton, J., Miller, P. A., Melton, J. R., Morino, I., Müller, J., Murguia-Flores, F., Naik, V., Niwa, Y., Noce, S., O'Doherty, S., Parker, R. J., Peng, C., Peng, S., Peters, G. P., Prigent, C., Prinn, R., Ramonet, M.,

https://doi.org/10.5194/egusphere-2026-3054
Preprint. Discussion started: 15 June 2026

Regnier, P., Riley, W. J., Rosentreter, J. A., Segers, A., Simpson, I. J., Shi, H., Smith, S. J., Steele, L. P., Thornton, B. F., Tian, H., Tohjima, Y., Tubiello, F. N., Tsuruta, A., Viovy, N., Voulgarakis, A., Weber, T. S., van Weele, M., van der Werf, G. R., Weiss, R. F., Worthy, D., Wunch, D., Yin, Y., Yoshida, Y., Zhang, W., Zhang, Z., Zhao, Y., Zheng, B., Zhu, Q., Zhu, Q., and Zhuang, Q.: The Global Methane Budget 2000–2017, Earth Syst. Sci. Data, 12, 1561–1623, https://doi.org/10.5194/essd-12-1561-2020, 2020.

Sawyer, C. F.: Washburn AL (1956) Classification of patterned ground and review of suggested origins. Geological Society of America Bulletin 67(7): 823–865, Progr. Phys. Geogr., 36, 440–448, https://doi.org/10.1177/0309133312436572, 2012.

Schad, P.: World Reference Base for Soil Resources—Its fourth edition and its history, J. Plant Nutr. Soil Sci., 186, 151–163, https://doi.org/10.1002/jpln.202200234, 2023.

Semrau, J. D., DiSpirito, A. A., and Yoon, S.: Methanotrophs and copper, FEMS Microbiol. Rev., 34, 496–531, https://doi.org/10.1111/j.1574-6976.2010.00212.x, 2010.

Smith, G. J., Angle, J. C., Solden, L. M., Borton, M. A., Morin, T. H., Daly, R. A., Johnston, M. D., Stefanik, K. C., Wolfe, R. G., Gil, B., and Wrighton, K. C.: Members of the genus Methylobacter are inferred to account for the majority of aerobic methane oxidation in oxic soils from a freshwater wetland, mBio, 9, e00815-18, https://doi.org/10.1128/mBio.00815-18, 2018.

Steinberg, L. M. and Regan, J. M.: mcrA-targeted real-time quantitative PCR method to examine methanogen communities, *Appl. Environ. Microbiol.*, **75**, 4435–4442, https://doi.org/10.1128/AEM.02858-08, 2009.

Tarnocai, C. and Zoltai, S. C.: Earth Hummocks of the Canadian Arctic and Subarctic, Arctic Alpine Res., 10, 581–594, https://doi.org/10.1080/00040851.1978.12003997, 1978.

Trotsenko, Y. A. and Khmelenina, V. N.: Aerobic methanotrophic bacteria of cold ecosystems, FEMS Microbiol. Ecol., 53, 15–26, https://doi.org/10.1016/j.femsec.2005.02.010, 2005.

Tveit, A. T., Hestnes, A. G., Robinson, S. L., Schintlmeister, A., Dedysh, S. N., Jehmlich, N., von Bergen, M., Herbold, C., Wagner, M., Richter, A., and Svenning, M. M.: Widespread soil bacterium that oxidizes atmospheric methane, P. Natl. Acad. Sci. USA, 116, 8515–8524, https://doi.org/10.1073/pnas.1817812116, 2019.

Vandenberghe, J.: Cryoturbation Structures, in: Encyclopedia of Quaternary Science, edited by: Elias, S. A., Elsevier, Amsterdam, 2147–2153, https://doi.org/10.1016/B0-44-452747-8/00109-5, 2007.

Van Vliet-Lanoë, B.: Frost and soils: implications for paleosols, paleoclimates and stratigraphy, Catena, 34, 157–183, https://doi.org/10.1016/S0341-8162(98)00087-3, 1998.

Voigt, C., Siljanen, H. M. P., Palacin-Lizarbe, C., Bennett, K. A., Chevrier-Dion, C., Fiencke, C., Knoblauch, C., Marquis, C., Marushchak, M. E., Saarela, T., Wilcox, E. J., and Sonnentag, O.: Contrasting methanotrophic communities between upland and polygonal tundra and their link to nitrogen metabolism and methane uptake in the Western Canadian Arctic, Soil Biol. Biochem., 213, 110038, https://doi.org/10.1016/j.soilbio.2025.110038, 2026.

Voigt, C., Virkkala, A.-M., Hould Gosselin, G., Bennett, K. A., Black, T. A., Detto, M., Chevrier-Dion, C., Guggenberger, G., Hashmi, W., Kohl, L., Kou, D., Marquis, C., Marsh, P., Marushchak, M. E., Nesic, Z., Nykänen, H., Saarela, T., Sauheitl, L., Walker, B., Weiss, N., Wilcox, E. J., and Sonnentag, O.: Arctic soil methane sink increases with drier conditions and higher ecosystem respiration, Nat. Clim. Change, 13, 1095–1104, https://doi.org/10.1038/s41558-023-01785-3, 2023.

Wang, M., Wang, S., Cao, Y., Jiang, M., Wang, G., and Dong, Y.: The effects of hummock-hollow microtopography on soil organic carbon stocks and soil labile organic carbon fractions in a sedge peatland in Changbai Mountain, China, Catena, 201, 105204, https://doi.org/10.1016/j.catena.2021.105204, 2021.

Washburn, A. L.: Classification of patterned ground and review of suggested origins, GSA Bull., 67, 823–866, https://doi.org/10.1130/0016-7606(1956)67[823:COPGAR]2.0.CO;2, 1956.

https://doi.org/10.5194/egusphere-2026-3054
Preprint. Discussion started: 15 June 2026

Washburn, A. L.: Permafrost features as evidence of climatic change, Earth-Sci. Rev., 15, 327–402, https://doi.org/10.1016/0012-8252(80)90114-2, 1980.

Wickham, H.: The split-apply-combine strategy for data analysis, J. Stat. Softw., 40, 1–29, https://doi.org/10.18637/jss.v040.i01, 2011.

Wickham, H.: ggplot2: elegant graphics for data analysis, Springer, New York, NY, USA, 2016.

Wilcox, E. J., Keim, D., de Jong, T., Walker, B., Sonnentag, O., Sniderhan, A. E., Mann, P., and Marsh, P.: Tundra shrub expansion may amplify permafrost thaw by advancing snowmelt timing, Arctic Sci., 5, 202–217, https://doi.org/10.1139/as-2018-0028, 2019.

Yao, X., Wang, J., and Hu, B.: How methanotrophs respond to pH: A review of ecophysiology, Front. Microbiol., 13, 1034164, https://doi.org/10.3389/fmicb.2022.1034164, 2023.

Yde, J. C. and Knudsen, N. T.: 20th-century glacier fluctuations on Disko Island (Qeqertarsuaq), Greenland, Ann. Glaciol., 46, 209–214, https://doi.org/10.3189/172756407782871558, 2007.

Zhao, J., Cai, Y., and Jia, Z.: The pH-based ecological coherence of active canonical methanotrophs in paddy soils, Biogeosciences, 17, 1451–1462, https://doi.org/10.5194/bg-17-1451-2020, 2020.

Zhuang, Q., Chen, M., Xu, K., Tang, J., Saikawa, E., Lu, Y., Melillo, J. M., Prinn, R. G., and McGuire, A. D.: Response of global soil consumption of atmospheric methane to changes in atmospheric climate and nitrogen deposition, Global Biogeochem. Cy., 27, 650–663, https://doi.org/10.1002/gbc.20057, 2013.

https://doi.org/10.5194/egusphere-2026-3054
Preprint. Discussion started: 15 June 2026

Appendix A

Table A1: Soil depth and chemical analyses Hummock H* and Non-hummocky tundra NH

SITE	HORIZON	AVERAGE DEPTH (CM)	PH (H_2O)	WATER CONTENT (%)	C (%)	N (%)	C:N
HUMMOCK	Oi	2.5	4.6	68.1	44.19	1.32	33.5
	Oe	7.5	4.3	73.2	38.25	1.65	23.2
	Oa	10.5	4.8	80.0	20.84	1.25	16.7
	Ah@1	18.0	6.0	54.8	9.82	0.72	13.6
	Ah@2	28.5	6.0	57.3	12.62	0.87	14.5
	AhBwl@1	47.0	6.6	20.6	2.34	0.17	13.8
	AhBwl@2	57.5	6.6	19.3	2.44	0.19	12.8
	AhBwl@3	67.0	6.6	22.1	2.72	0.21	13.0
	BwlAh@f	85.0	6.9	20.6	0.96	0.07	13.7
NON-HUMMOCKY TUNDRA	Oe	5	5.7	85.0	45.09	1.36	33.2
	Oa	16	5.8	79.3	34.13	1.83	18.7
	Ahg	31	5.6	38.8	6.47	0.4	16.0
	Ahgf	50	5.9	50.5	4.89	0.32	15.2

https://doi.org/10.5194/egusphere-2026-3054
Preprint. Discussion started: 15 June 2026

Appendix B

Appendix Table B1: *mcrA* copy numbers in the different NH replicates. nd=not detected, nm =not measured

775

NH REPLICATE	DEPTH (CM)	QPCR_MCRA COPY NUMBERS PER G DW
1	0-7	nd
1	7-12	nd
1	12-19	112114.95
1	19-37	nd
1	37-39	271768.944
2	0-8	108101.061
2	8-21	22919927.9
2	21-34	nd
2	34-47	70871.1733
3	0-3	nm
3	3-15	nm
3	15-29	nm
3	29-44	nm

https://doi.org/10.5194/egusphere-2026-3054
Preprint. Discussion started: 15 June 2026

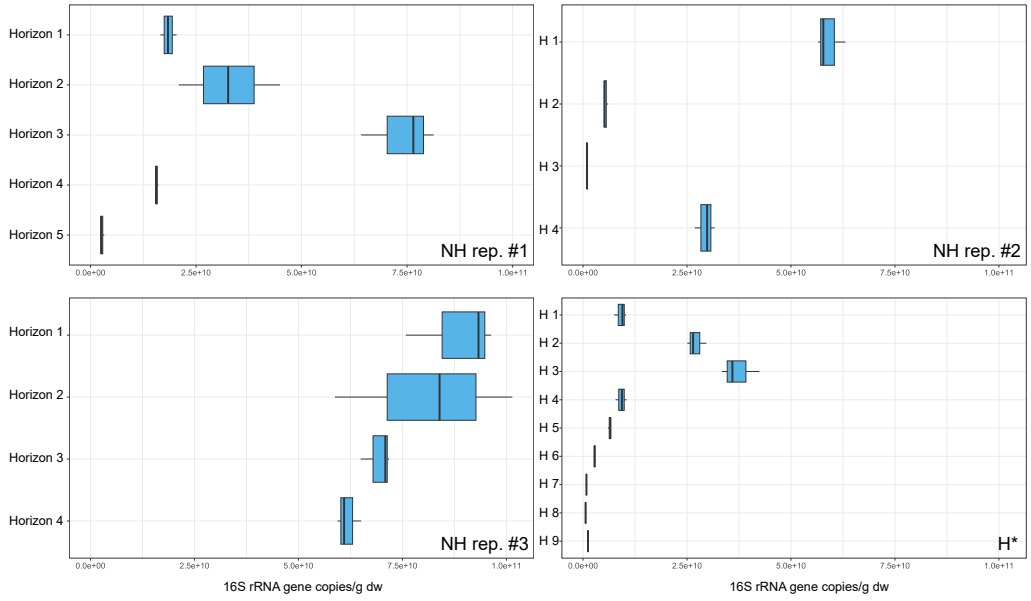

Appendix Figure B1: Bacterial 16S rRNA gene qPCR results of all replicates of NH in comparison with H*.

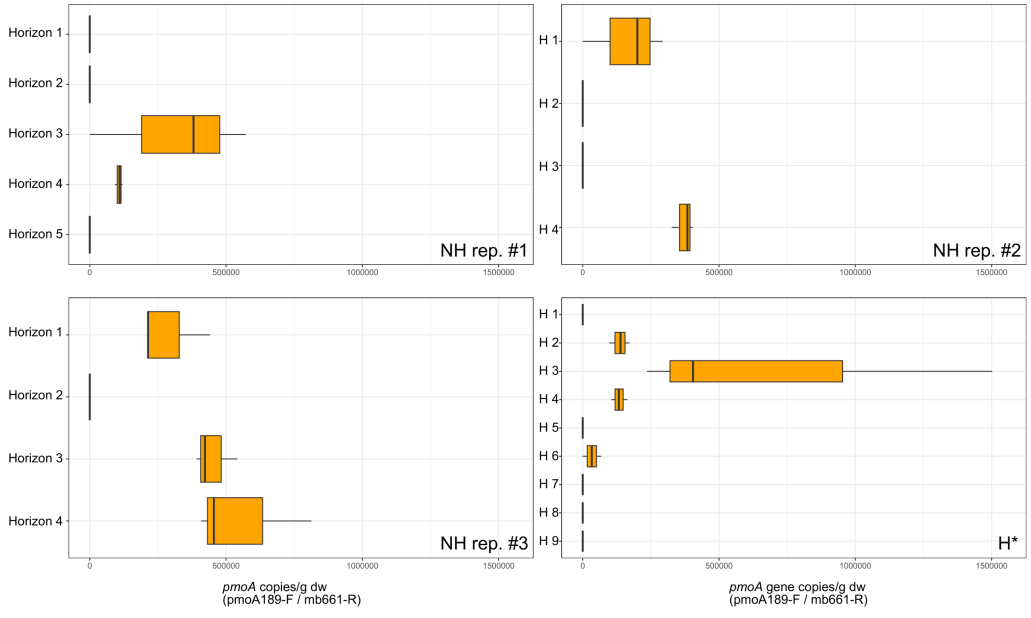

Appendix Figure B2: pmoA qPCR results of all replicates of NH in comparison with H*, achieved with the primer combination pmoA 189-F/mb650-R.

https://doi.org/10.5194/egusphere-2026-3054
Preprint. Discussion started: 15 June 2026

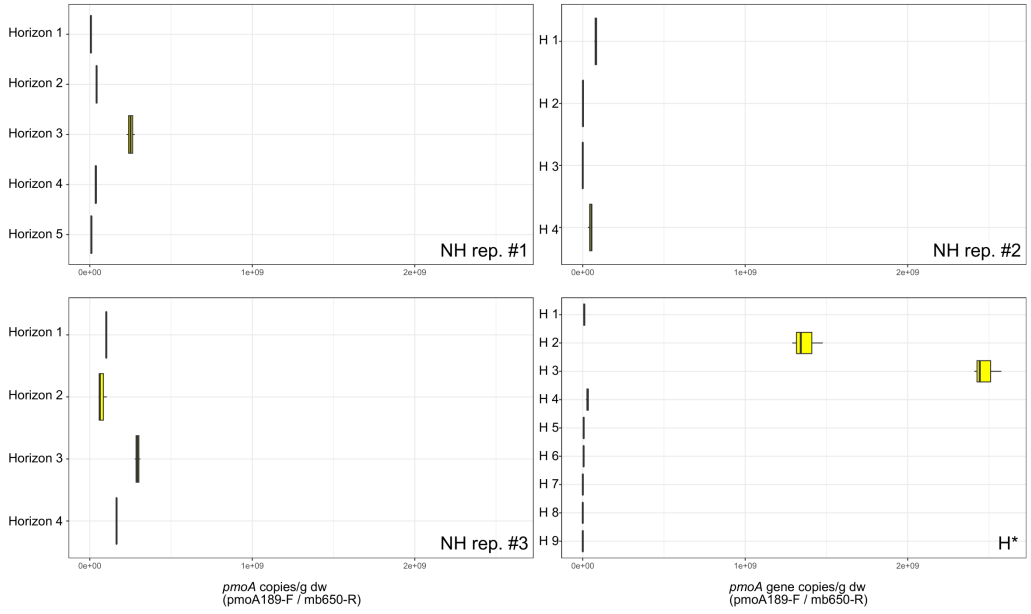

Appendix Figure B3: pmoA qPCR results of all replicates of NH in comparison with H*, achieved with the primer combination pmoA 189-F/mb650-R.

790

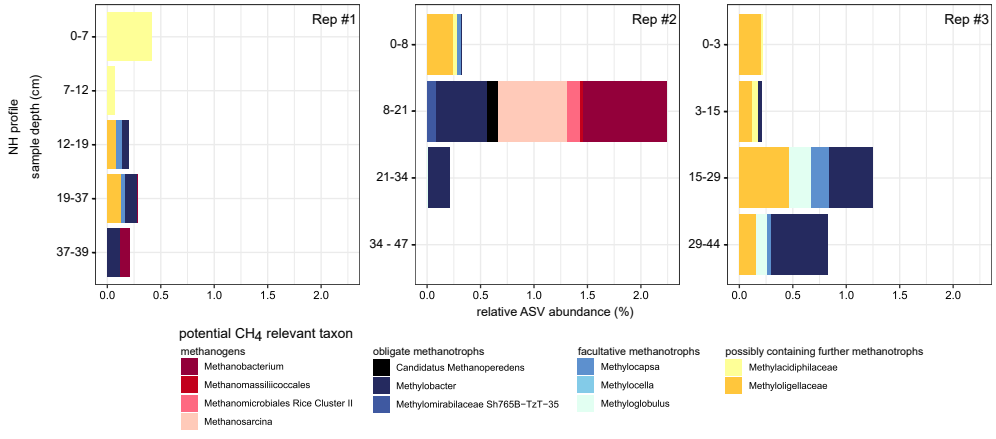

Appendix Figure B4: Amplicon-results of potentially methane relevant prokaryotes in all NH replicates. Replicate #2 was the only

795